DRDC Ottawa SL 2002-164

X-band wideband experimental airborne radar for SAR, GMTI and maritime surveillance

A. Damini, M. McDonald and G.E. Haslam

Abstract: Defence Research and Development Canada - Ottawa has completed Phase I in the development of a new multimode X-band wideband experimental airborne radar (XWEAR) to support studies in synthetic aperture radar (SAR) imaging, inverse SAR (ISAR), ground moving target indication (GMTI) radar and maritime surveillance radar with particular focus on small target detection and long-range surface surveillance. Specific areas of interest include research into SAR imaging techniques for fixed and moving targets, time–frequency analysis of ocean and land moving targets, space–time adaptive processing for application to GMTI, investigation into the electromagnetic backscatter properties of the ocean surface, generation of signatures for automatic target recognition and feature extraction, and analysis on the immunity of wide bandwidth systems against electronic countermeasures. Phase I culminated with the flight trialling of the SAR and maritime surveillance modes. Phase II will see the trialling of the wide area surveillance GMTI (WAS GMTI) and integrated SAR–GMTI modes. A description of the experimental radar is given along with an overview of its data collection capability. Distinguishing features include operation at X-band, single-channel operation for SAR and maritime surveillance, and two-channel operation for WAS-GMTI and integrated SAR–GMTI. The new radar maximises the use of an existing digital scan converter as a controller, and commercially available components including the transmitter, A/D converters and computer boards. The timing circuitry, waveform generator, single- and dual-channel receivers are custom built.

List of acronyms

A/D	analogue-to-digital
APC	antenna phase centre
CPI	coherent processing interval
DAS	data acquisition system
DSC	data scan controller
EGI	embedded global positioning/inertial navigation system
GMTI	ground moving target indication
IF	intermediate frequency
IMU	inertial measurement unit
ISAR	inverse synthetic aperture radar
PPI	plan position indication
PRI	pulse repetition interval
RAID	redundant array of inexpensive discs
RAS	range–azimuth sector
RF	radio frequency
RXP	receiver–exciter processor
SAR	synthetic aperture radar
WAS	wide area surveillance
XWEAR	X-band wideband experimental airborne radar
ZRT	zero-range trigger

IEE Proceedings online no. 20030654

doi: 10.1049/ip-rsn:20030654

Paper first received 16th December 2002 and in revised form 22nd May 2003

The authors are with Radar Systems, Defence Research and Development Canada - Ottawa, 3701 Carling Avenue, Ottawa, Ontario, Canada K1A 0Z4

1 Introduction

The rapid evolution of electronic components is allowing smaller, lighter and more versatile radar systems to be developed within increasingly tight budgets and time constraints. The X-band wideband experimental airborne radar (XWEAR) was developed as an air-to-surface sensor that can record large volumes of data for investigations into wideband SAR, ISAR, GMTI and maritime surveillance. It supplies a multimode experimental radar testbed that can collect data for research into SAR imaging techniques for fixed and moving targets, time–frequency analysis of ocean and ground moving targets, space–time adaptive processing for application to GMTI, investigations into the electromagnetic backscatter properties of the ocean surface, generation of signatures for feature extraction and automatic target recognition studies, and analysis of the immunity of wide bandwidth systems against electronic countermeasures. X-band, because of its relative immunity to tropospheric effects, allows operation in the maritime environment to ranges of 200 nmi. Phase I of the XWEAR programme was completed with the successful flight trialling of the SAR and maritime surveillance modes with the radar installed on a Convair 580 aircraft.

The architecture of the experimental radar is described along with its most salient system level and data collection capability characteristics. The detection performance of the maritime surveillance modes is modelled from the design parameters, and results from the flight trials against ocean targets of opportunity are presented. For the SAR modes, preliminary imagery from both land and ships are presented. Land-based SARs typically target static positions and may require a refocusing of the data to image ground moving

targets. Sea-based SARs target ocean-going vessels which may, or may not, have their own translational and rotational components of motion. Sea-based SARs generally fly at lower altitudes than land-based systems and thus may require motion compensation which is more sophisticated for operation in turbulent environments. XWEAR is designed as both a land- and sea-based SAR system.

2 Experimental radar description

A block diagram of the radar system architecture is shown in Fig. 1. The data scan controller (DSC) is a digital scan converter designed for the AN/APS-506 search radar that has been modified for SAR and GMTI control. The antenna servo and power supply are also taken from the AN/APS-506 maritime surveillance radar. The Raytheon transmitter is capable of transmitting 50 kW pulses of up to 30 μs duration with a maximum duty cycle of 1%. The navigation subsystem consists of a Litton LR-86 inertial measurement unit (IMU) mounted near the antenna phase centre (APC) and a Honeywell H-764G embedded global positioning/inertial navigation system (EGI) mounted near the centre of gravity of the aircraft. The receiver–exciter processor (RXP) is a new subsystem central to the experimental radar.

The functionality of the RXP is derived from a blend of hardware and software functions. Hardware-dependent functions comprise waveform generation, radar system timing, radar up/down conversion and analogue-to-digital conversion. Software-dependent functions include system control, targeting, navigation, motion compensation and radar system timing control, radar data recording and the operator interface for coherent radar data acquisition. The radar system timing circuitry and radar front end are designed specifically for this radar. All timing and local oscillator signals for waveform generation, radar up-conversion, radar down-conversion and signal digitisation are derived from the RXP's low-phase noise reference clock. An arbitrary waveform generator is employed to generate highly precise linear frequency modulated waveforms of various bandwidths, from files containing digital waveform descriptions, to modulate the intermediate frequency (IF) signal. The RXP up-converts this IF waveform to the transmitter radiofrequency (RF) of 9.75 GHz. The system's spurious free dynamic range exceeds 45 and 65 dB for the widest bandwidth SAR modes and the narrowband wide-area surveillance modes, respectively. The RXP receives the EGI data as well as target data from the DSC via a 1553B interface. A custom interface brings the IMU data into the RXP. The RXP timestamp clock and reset are derived from the DSC. In the receiver, the RF echo is mixed with a local oscillator of 9.25 GHz to produce a down-converted signal at an IF of 500 MHz. Eight bit analogue-to-digital conversion is performed on the IF signal at rates up to two GHz in the single channel modes and up to 14 bits/channel at maximum rates of 100 MHz in the two-channel modes. The RXP sends the digitised IF data to the 144 Gbyte redundant array of inexpensive discs (RAID) for recording at rates up to 65 MBytes/s.

A summary of the characteristics of the radar is given in Table 1. Table 2 lists the data collection modes and characteristics of the corresponding recorded data. In the single-channel modes, 32768 eight-bit samples are digitised per PRI. For each channel in the two-channel modes, 8192 14-bit samples are digitised per PRI. Seaspot is a spotlight SAR imaging mode in which the radar illuminates an ocean target such as a ship. Landspot is the corresponding term for land targets. Table 1 summarises the range resolutions that are supported. The range resolutions listed assume no degradation in the main-lobe response due to window weightings imposed on the pulse compression filter.

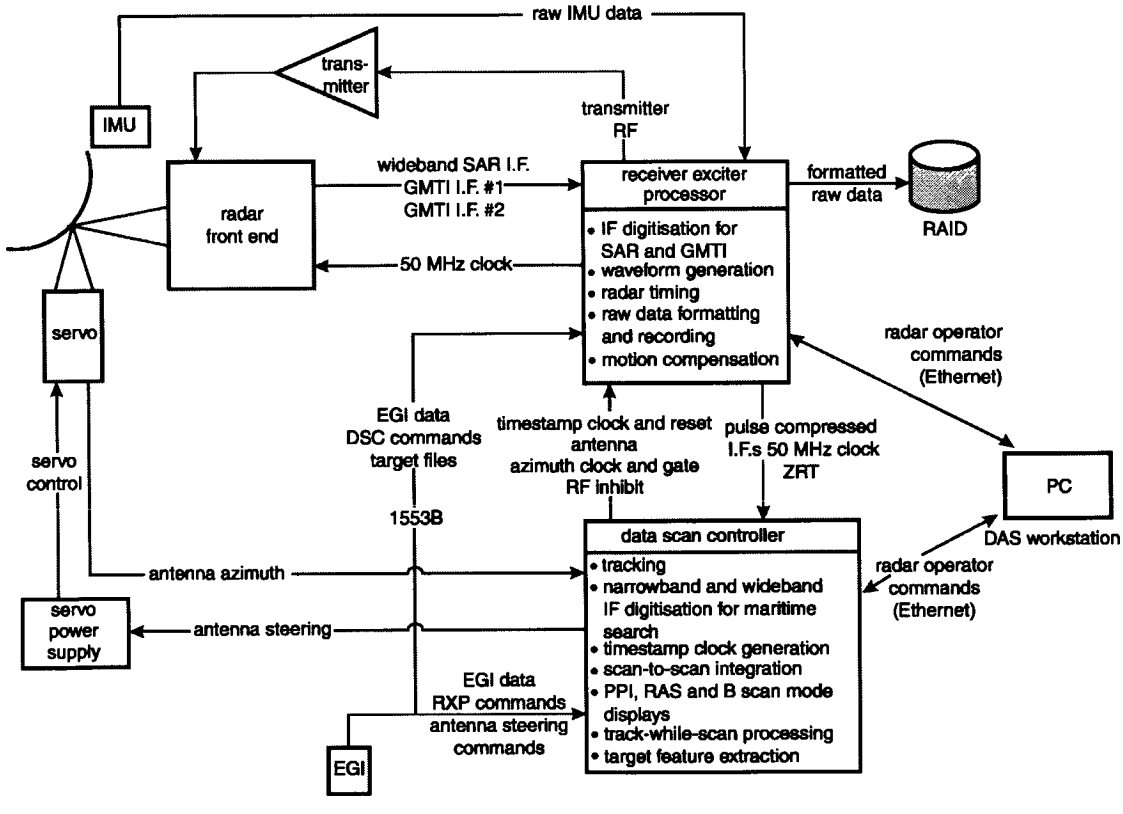

Fig. 1 *Experimental airborne radar architecture*

Table 1: Radar system parameters

Pulse length	5 μs in all modes except Search II which is 10 μs with a fixed 5 MHz signal that randomly frequency hops over a 500 MHz range
Peak power	50 kW
Carrier frequency	9.75 GHz
Polarisation	Transmit–horizontal/receive–horizontal
Antenna	42" width, 2.4° azimuth beamwidth, 4.0° elevation beamwidth
Range resolution	As noted in Table 2, otherwise <1 m

Table 2: Radar data collection modes

Mode	Antenna control	PRF Hz	Range resolution m	Samples per swath/ bits per sample
Search I (full scan or gated sector on designated target)	DSC controlled 300 RPM full scan or gated sector (ground stabilised), RXP controls range gate delay for digitisation	2000	0.3	32 768/8
Search II (full scan or sector scan on designated target)	DSC controlled 6 RPM sector (ground stabilised) or full scan, RXP controls range gate delay for digitisation	500	30	16 384/8
Search III (full scan or sector scan on designated target)	DSC controlled 6 RPM sector (ground stabilised) or full scan, RXP controls range gate delay for digitisation	500	0.3	32 768/8
Search IV (full scan or gated sector on designated target)	DSC controlled 60 RPM full scan or gated sector (ground stabilised), RXP controls range gate delay for digitisation	400	0.3	32 768/8
Single channel strip	RXP controlled antenna pointing	100 to 1375	<1, 1.3	32 768/8
Single channel land spot	RXP controlled antenna pointing	100 to 1375	<1, 1.3	32 768/8
Single channel sea spot	RXP controlled antenna pointing	500	<1, 1.3	32 768/8
Two-channel strip (SAR–GMTI)	RXP controlled antenna pointing	100 to 1375	5, 10	2 × 8192/14
Two-channel land spot (SAR–GMTI)	RXP controlled antenna pointing	100 to 1375	5, 10	2 × 8192/14
Two-channel sea spot	RXP controlled antenna pointing	500	<1	2 × 8192/14
WAS–GMTI	RXP controlled 6 RPM narrow or wide sector scan, with/without ground stabilisation	2000	5, 10	2 × 8192/14

3 Coherent data acquisition design

Coherent integration over a long synthetic aperture or coherent processing interval (CPI) requires that the radar data be compensated for undesirable APC motion that introduces pulse-to-pulse phase errors [1]. Spurious motion generally results from changes in aircraft ground speed and deviation of the actual flight track from the ideal track. The RXP is specifically designed to collect coherent radar echo data. Figure 2 outlines the RXP design with respect to its capability to perform coherent data acquisition [2]. The functions of navigation and motion compensation are more specifically described in terms of strapdown navigation and Kalman filtering. Figure 2 also includes a placeholder for the signal processing of the radar echo data. The signal processing is currently performed in a postflight environment, however there is provision in the RXP design to retrofit it with onboard SAR, GMTI and coherent maritime surveillance signal processing.

The APC motion is measured by the IMU that is situated on the roll/pitch-stabilised antenna ring gear close to the APC location. The IMU provides high-rate (200 Hz) measurements in the form of velocity increments and angular increments that are subsequently processed by strapdown navigator algorithms to yield estimates of APC position and velocity, and antenna orientation. The EGI provides estimates of aircraft position and velocity, and aircraft orientation (roll, pitch and heading) at the EGI mounting site. The EGI information is derived from blending inertial data with GPS data in a Kalman filter that is internal to the EGI. The accuracy of the EGI position and velocity estimates is specified to be 16 m (spherical error probability) and 0.03 m/s (RMS), respectively. The EGI data are used in a transfer-of-alignment Kalman filter, implemented in the RXP software, to estimate long-term errors in the strapdown navigation data that result from inaccuracies in the IMU accelerometers and gyroscopes. The strapdown navigation, Kalman filtering and targeting

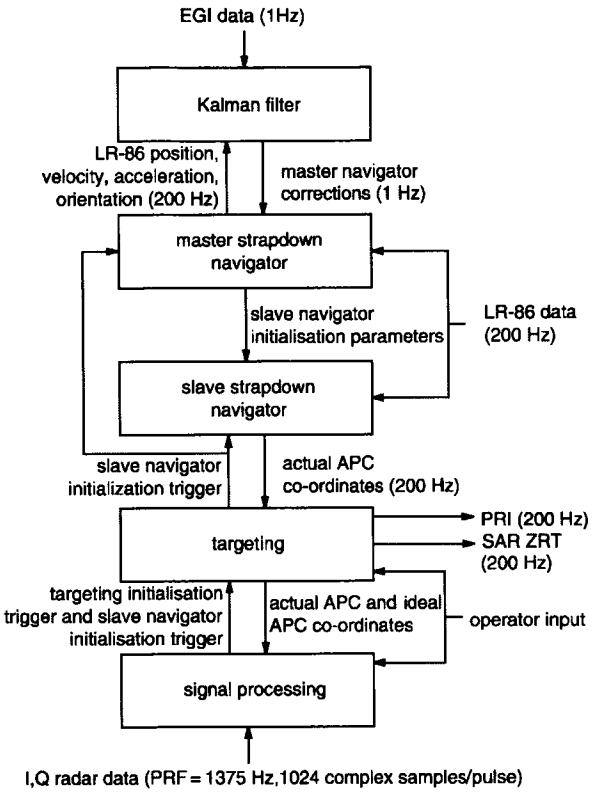

Fig. 2 *RXP design for coherent data acquisition*

modules from Fig. 2 are further discussed in the following Sections.

3.1 Strapdown navigation

The strapdown navigation module consists of two identical strapdown navigator algorithms that are designated as master and slave. The master navigator runs continuously, producing estimates of APC position and velocity, along with antenna orientation, at a 200 Hz rate, based on the LR-86 IMU data. These quantities are corrected at a 1 Hz rate using estimates of the strapdown position, velocity and attitude errors provided by the transfer-of-alignment Kalman filter. At the beginning of data collection, a slave navigator is launched in parallel with the master navigator. The slave navigator position, velocity and attitude are initialised with master navigator estimates at that point in time. During SAR imaging, the master and slave navigators process the same IMU input data, but the quantities computed by the slave navigator are not updated with the Kalman filter error estimates. The slave navigator quantities are ultimately used to compute the radar phase corrections, as well as PRI and digitisation window adjustments. The use of the update-free slave navigator data for this purpose ensures that there are no step changes in the time history of the computed radar corrections, which tend to create undesirable image artefacts. To apply the phase corrections, it is necessary to buffer the time-stamped radar data and to interpolate the phase corrections to the corresponding time of emission of each pulse. Similarly, to account for the inevitable latency in producing the Kalman filter results, extrapolation is used to calculate the PRIs.

3.2 Kalman filtering

The motion compensation Kalman filter contains 15 strapdown error states, comprising three position errors, three velocity errors, three platform misalignments (attitude errors), three accelerometer biases and three gyroscope biases. The Kalman filter measurements are derived by differencing EGI position and velocity quantities with corresponding quantities from the master strapdown navigator after lever arm corrections have been applied to refer the EGI and strapdown navigation data to the same point in space. The Kalman filter processes these measurements at a 1 Hz rate to update its error state estimates, which are then used to correct the master strapdown navigation quantities in a closed-loop fashion. Control of strapdown platform misalignments are of particular concern, especially in the presence of significant air turbulence [3].

3.3 Targeting

The functions performed by the targeting module include; translation of operator inputs into the appropriate radar mode initialisation parameters, transformation of the strapdown navigation data from a navigation frame to an appropriate targeting frame, and calculation of updated radar PRI values and digitisation window adjustments to be applied during radar data collection. Targeting is initialised by a signal originating from the operator interface to signal processing at the start of any conventional radar data collection session. The targeting instructions in the various modes are specified as follows:

Landspot: geodetic latitude, longitude and elevation in metres
Seaspot: a single target to image, either tracked by the DSC track-while-scan or directly from the PPI display on the DSC
Stripmap: two target locations in terms of geodetic latitude, longitude and elevation, and the centre of the swath is calculated so as to pass through the two specified targets (this allows for off-track stripmap imaging while maintaining the finest resolution allowed by the bandwidth of the antenna)
WAS-GMTI: a ground-stabilised sector on the ground in terms of geodetic latitude, longitude and elevation; or a moving sector on the ground in terms of target range in metres, azimuth angle off the aircraft nose and elevation
Search I to IV: a ground-stabilised sector, the centre of which is either a tracked target or chosen directly from the PPI display on the DSC; a ground-stabilised sector on the ground in terms of geodetic latitude, longitude and elevation; or a full scan with a fixed range and antenna tilt

In both WAS–GMTI and the maritime search modes the sector width is specified in 20° increments up to 140°. In all modes, the operator specifies the number of pulses to record.

The targeting function fixes the PRI in the WAS-GMTI, SAR–GMTI and maritime search modes. For the SAR modes, it computes the updated PRI as a function of both the aircraft velocity component along the ideal flight track and the desired antenna squint. This results in the radar pulses being transmitted at equispaced intervals along the desired track. The pulse repetition frequency is thus formulated as $PRF = S_s V \sin(\eta)$, where S_s is the spatial sampling constant of 5.3333 Hz/(m/s), V is the magnitude of the APC velocity vector and η is the squint angle. η is measured clockwise from the nose of the aircraft. The digitisation window adjustments computed by the targeting module are used to control the triggering of the zero-range trigger (ZRT) so as to maintain the centre of the digitisation window over the area being imaged regardless of aircraft deviation from the desired track. Likewise, antenna steering is controlled to maintain the required Doppler centroid during illumination. APC position and velocity information that has been transformed to the targeting frame is forwarded to the signal processing software. This information is particularly

important in the SAR modes where the signal processing software uses it to compute the phase corrections required to modulate the phase of the sampled radar data, on a pulse-to-pulse basis, so that the echo data from a target at the centre of the imaged patch appears to have been collected with the APC following the ideal path. An autofocus step is used to correct for undesirable aircraft motions not compensated for by the motion compensation, as well as residual low-frequency errors inherent in the slave strapdown navigation data.

4 Performance

The radar was flight trialled in the single-channel modes, maritime search and SAR, in November 2002. In the following, the predicted and demonstrated performance obtained by the radar in the maritime search modes are presented. Examples of images generated from the ocean target and land imaging SAR modes are also presented.

4.1 Maritime search performance analysis

The DSC gives the experimental radar system a real-time surveillance capability for detecting large and small targets. This capability is essential for the effective collection of ocean data as the PPI display and track-while-scan capability provide the operator with real-time feedback on target locations and the general behaviour of the returns within the areas under surveillance. This allows the operator to efficiently tailor the data collection parameters to the scene at hand. Table 2 outlines the various data collection modes of the radar. In particular, the high-resolution modes corresponding to Search I, III and IV provide the operator with the ability to locate small targets such as periscopes or small boats buried in sea clutter. In Search I, III and IV, the DSC employs a peak detection scheme which extracts the peak measured values within a specified range interval from the IF signal and displays them to the screen for subsequent scan-to-scan integration. Despite the simplicity of the detection method, the excellent RF performance of the radar front end and the low noise figure yield good long-range detection performance.

The anticipated small target detection performance of the DAS has been modelled for both a $1\,m^2$ and a $5\,m^2$ cross-section, Swerling 1 target in sea-state 3 for a platform altitude of 500 ft. The results are shown in Figs. 3*a* and 4*a*, respectively. Clutter returns are simulated using the GIT clutter model [4] and the empirical shape parameter model of Watts *et al.* [5, 6]. A downwind viewing direction is assumed. In both Figures a short-range detection 'hole' due to the strong clutter returns and increased spikiness

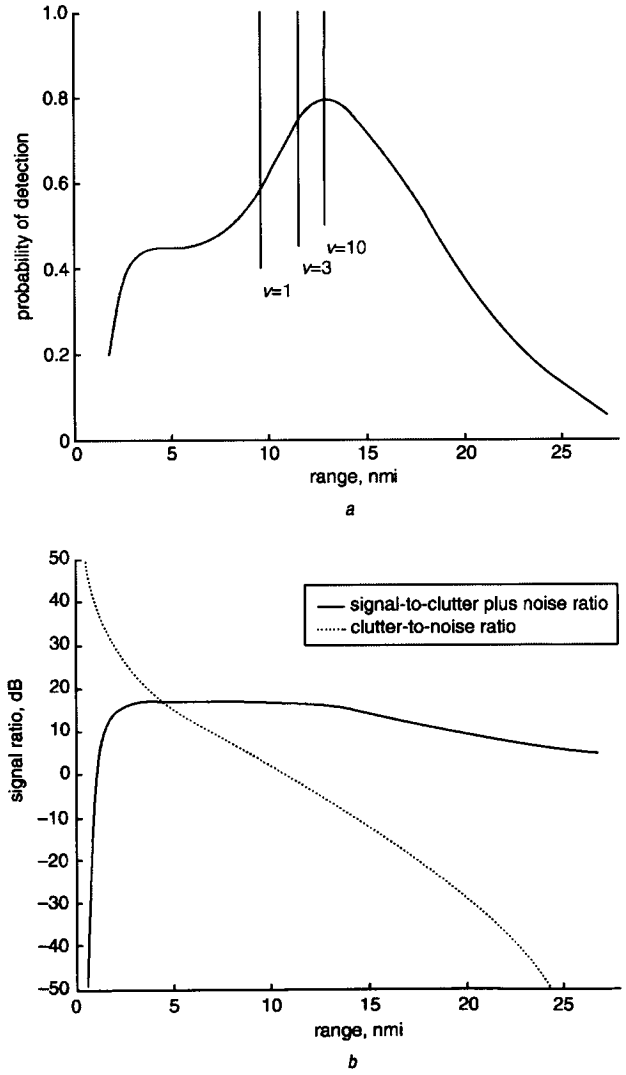

Fig. 3 *Performance calculations for $1\,m^2$ Swerling 1 target in sea-state 3 conditions from airborne platform at 500 ft*

a Probability of detection against range
b Signal-to-clutter plus noise ratio and clutter-to-noise ratio

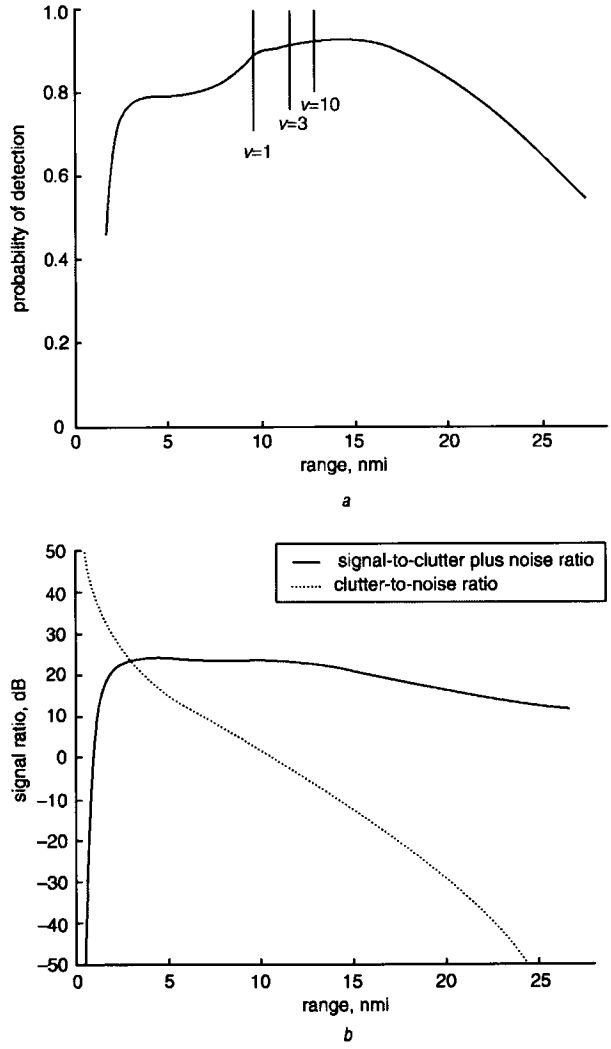

Fig. 4 *Performance calculations for $5\,m^2$ Swerling 1 target in sea-state 3 conditions from airborne platform at 500 ft*

a Probability of detection against range
b Signal-to-clutter plus noise ratio and clutter-to-noise ratio

(i.e. smaller shape parameter) at steeper angles of incidence is readily apparent. The range locations at which K distribution shape parameters of 1, 3 and 10 are reached are also shown. Figures 3*b* and 4*b* show the calculated signal-to-clutter plus noise and signal-to-clutter ratios for the 1 m^2 and 5 m^2 targets, respectively. It is easily seen that at short ranges the signal-to-clutter plus noise is dominated by clutter, but becomes noise-limited at long ranges.

Figure 3*a* indicates that a 1 m^2 target remains detectable out to approximately 17 nautical miles. Increasing the target cross-section to 5 m^2, Fig. 4*a*, extends the detectability range out to the radar horizon at approximately 27 nautical miles. These results are approximate as they represent a highly idealised representation of the real noise and clutter environments, but they nevertheless give an indication of the sensitivity of the radar. The good long-range detection performance in the noise-limited portion of the radar echo return is a direct result of the low noise figure of the radar receiver.

4.2 Maritime search performance

The high resolution of the radar also provides the potential for range profiling of extended targets. Figures 5*a* and 5*b* present range profiles of two different ships collected using the experimental radar system. Figure 5*a* corresponds to a large merchant vessel and Fig. 5*b* to a smaller marine craft (the corresponding SAR images are presented in Fig. 8). The extended return from the large vessel, Fig. 5*a*, is clearly observed in the range profile and an estimate can be formed of the overall length from the profile. In addition the relative location of several strong returns from the ship structure can also be observed and could be used as an aid in ship classification. The small craft range profile, Fig. 5*b*, does not produce the clear extended return observed with the larger merchant vessel, rather a pair of strong localised returns is observed. Nevertheless, the shorter length of this craft in comparison with the larger vessel is readily observed.

4.3 SAR Results – land imaging and time–frequency analysis for ship imaging

The performance of the system in its SAR imaging mode is best quantified by analysis of imagery formed of fielded corner reflectors. Figure 6*a* is a stripmap image of an urban area. Figure 6*b* is a stripmap image of an array of five corner reflectors. In the field to the left of the corner reflectors are bales of hay (shadows evident). Figures 7*a* and 7*b* are the range and azimuth impulse responses of one of the corner reflectors in Fig. 6*b*. The SAR data was processed to pixel resolutions of 1 m for presentation purposes and the image pixels were subsequently resampled to 0.3 m for display. The −3 dB width of the experimental performance is seen to meet the theoretical results.

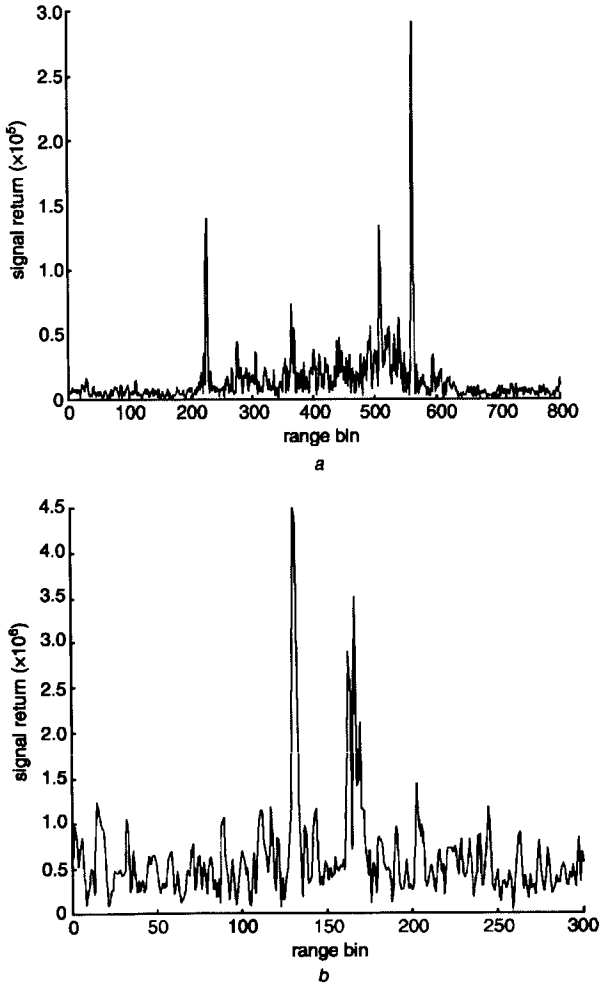

Fig. 5 *Range profiles*
a Large merchant vessel
b Small marine craft

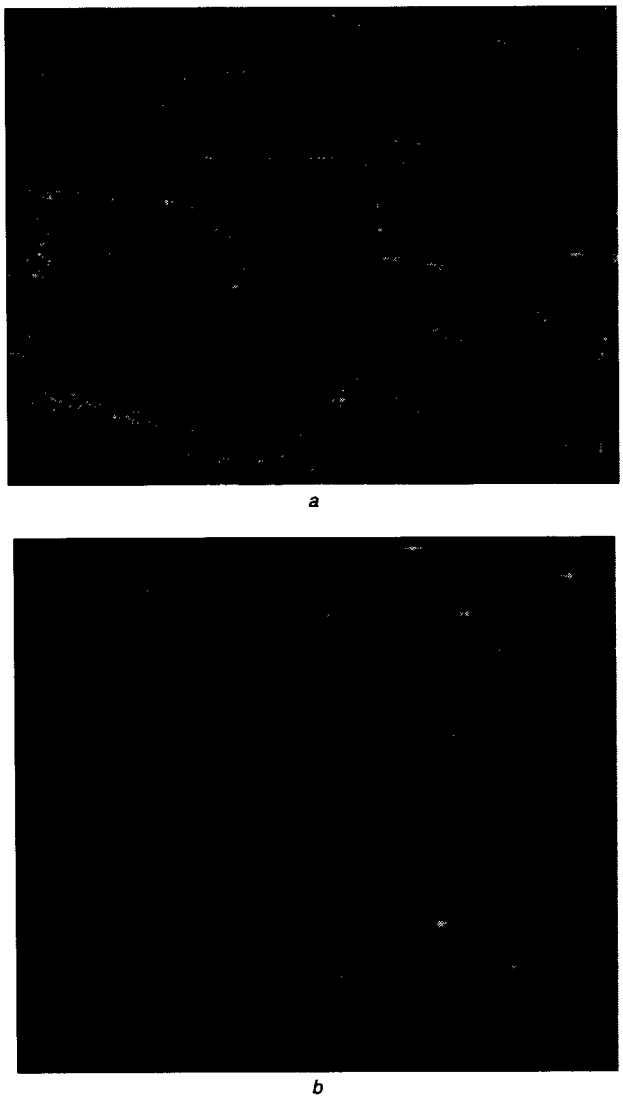

Fig. 6 *Stripmap imagery (range along vertical)*
a Wide swath of urban area
b Zoom-in on a field of corner reflectors

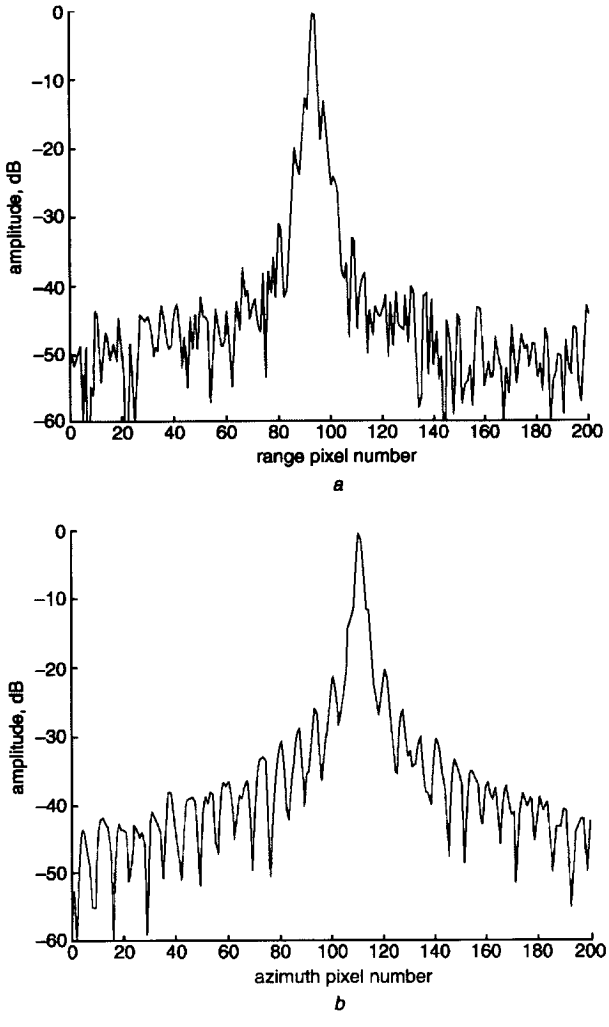

Fig. 7 *Cross-sections of corner reflector*
a Range
b Azimuth

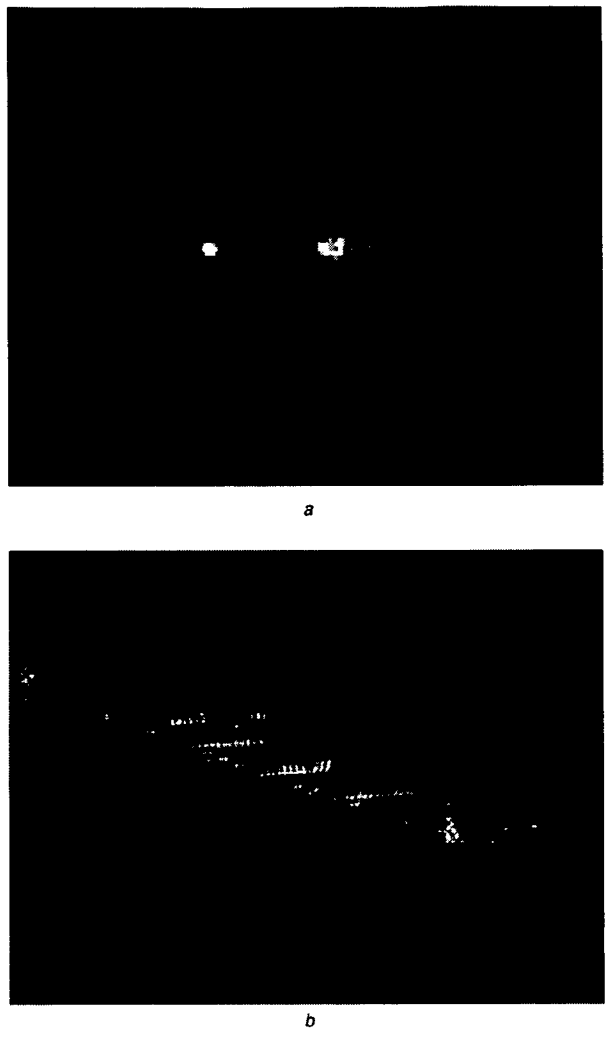

Fig. 8 *Seaspot image*
a Small marine craft
b Large merchant vessel

Hybrid SAR/ISAR ship imaging involves the imaging of a target that has its own components of motion. The signal processing for this is traditionally decoupled into two one-dimensional tasks, since the motion of the target in each direction is unknown. The seaspot algorithm performs range compression and tracking in the range direction (multiple targets are tracked and corrected as opposed to using a deterministic range cell migration correction process, such as that traditionally employed in spotlight SAR). In the cross-range (Doppler) direction, the target may be undergoing complex rotational motions thus information about its frequency content cannot be obtained using traditional waveform analysis such as a single fast Fourier transform. Time–frequency analysis allows the time and frequency information to be viewed simultaneously. A short-time Fourier transform (subapertures around 64 ms) is used to provide good time domain resolution while avoiding distortion of the frequency spectrum. Heavy overlapping (around 50%) of the time domain windows is used to recover as much information as possible on the target. One or more targets are then tracked in Doppler and cost functions are applied to estimate the optimal location and length of a subset within the original aperture for final image formation. The same targets are then corrected in the Doppler domain to allow coherent subaperture processing to be used to integrate the data in azimuth and form the final image. The orientation of the image projection plane of the resulting image is generally unknown, but analytical studies have been shown to correspond to experimental results obtained by instrumenting vessels to measure their motion and comparing the resulting seaspot imagery to the image orientations predicted from the measured motion [7, 8]. Figure 8 presents seaspot images of targets of opportunity. Figure 8*a* is a small craft and Fig. 8*b* is an unknown merchant vessel.

5 Concluding remarks and looking ahead

Phase I of XWEAR was successfully flight tested in November 2002. SAR data were collected in the land and ocean surveillance modes. Maritime search data were also collected for continuing studies in coherent small target detection. Imagery from the flight testing of the SAR modes in the land imaging and ship imaging modes were presented as well as range profiles illustrating performance in the maritime environment. Analysis of XWEAR data is continuing to assess the capability of its wideband operation at X-band and frequency agility in the maritime surveillance modes. Future radar trials are being planned to collect additional data for studies, including ground moving target imaging, feature extraction from ground moving targets, automatic target recognition and electronic counter-counter measures.

In 2003, during Phase II of XWEAR, the antenna will be modified for a two-channel capability and the experimental

radar trialled in the two-channel SAR–GMTI and WAS GMTI modes. Phase II will demonstrate the feasibility of implementing a surveillance system capable of both land and maritime surveillance/imaging of fixed and moving targets within a single radar.

6 References

1 Haslam, G.E., and Damini, A.: 'Specifying the allowable latencies in the application of SAR motion corrections'. Proc. EUSAR '96, European Conf. on Synthetic aperture radar, Konigswinter, Germany, 26–28 March 1996, pp. 403–406

2 Damini, A., and Difilippo, D.J.: 'An integrated motion compensation/SAR signal processor for the spotlight SAR ADM'. Proc. EUSAR '98, European Conf. on Synthetic aperture radar, Freidrichshafen, Germany, 25–27 May 1998, pp. 107–110

3 Difilippo, D.J., Haslam, G.E., and Widnall, W.S.: 'Evaluation of a Kalman filter for SAR motion compensation'. Proc. IEEE PLANS 88, Orlando, FL, USA, November 1988, pp. 259–268

4 Horst, M.M., Dyer, F.B., and Tuley, M.T.: 'Radar sea clutter model', URSI Digest, Int. IEEE AP/S URSI Symposium, 1978, pp. 6–10

5 Watts, S., and Wicks, D.C.: 'Empirical models for detection prediction in K-distribution radar sea clutter'. Proc. IEEE Int. Radar Conf., Arlington, VA, USA, 1990, pp. 189–194

6 Watts, S.: 'A practical approach to the prediction and assessment of radar performance in sea clutter'. Proc. IEEE Int. Radar Conf., Alexandria, VA, USA, 1995, pp. 181–186

7 Godbole, P., Damini, A., and Haslam, G.E.: 'Instrumented ship imaging experiment using the AN/APS-506 Spotlight SAR System'. Proc. 4th Int. Airborne Remote Sensing Conf. and Exhibition, Ottawa, Canada, 21–24 June 1999, pp. 272–279

8 Damini, A., and Haslam, G.E.: 'SAR/ISAR ship imaging: Theoretical analysis and practical results'. Proc. EUSAR '96, European Conf. on Synthetic aperture radar, Konigswinter, Germany, 26–28 March 1996, pp. 443–446